

Research



Cite this article: Page MT, Garcia-Becerra T, Smith AG, Terry MJ. 2020 Overexpression of chloroplast-targeted ferrochelatase 1 results in a *genomes uncoupled* chloroplast-to-nucleus retrograde signalling phenotype. *Phil. Trans. R. Soc. B* **375**: 20190401. <http://dx.doi.org/10.1098/rstb.2019.0401>

Accepted: 24 January 2020

One contribution of 20 to a theme issue 'Retrograde signalling from endosymbiotic organelles'.

Subject Areas:

plant science, cellular biology

Keywords:

haem, plastid signalling, tetrapyrroles, mitochondria, *gun* phenotype

Author for correspondence:

Matthew J. Terry

e-mail: mjt@soton.ac.uk

[†]Present address: Lancaster Environment Centre, Lancaster University, Lancaster LA1 4YQ, UK.

Electronic supplementary material is available online at <https://doi.org/10.6084/m9.figshare.c.4927767>.

Overexpression of chloroplast-targeted ferrochelatase 1 results in a *genomes uncoupled* chloroplast-to-nucleus retrograde signalling phenotype

Mike T. Page^{1,†}, Tania Garcia-Becerra¹, Alison G. Smith² and Matthew J. Terry¹

¹School of Biological Sciences, University of Southampton, Highfield Campus, Southampton SO17 1BJ, UK

²Department of Plant Sciences, University of Cambridge, Downing Street, Cambridge CB2 3EA, UK

id MTP, 0000-0002-9715-7076; AGS, 0000-0001-6511-5704; MJT, 0000-0001-5002-2708

Chloroplast development requires communication between the progenitor plastids and the nucleus, where most of the genes encoding chloroplast proteins reside. Retrograde signals from the chloroplast to the nucleus control the expression of many of these genes, but the signalling pathway is poorly understood. Tetrapyrroles have been strongly implicated as mediators of this signal with the current hypothesis being that haem produced by the activity of ferrochelatase 1 (FC1) is required to promote nuclear gene expression. We have tested this hypothesis by overexpressing FC1 and specifically targeting it to either chloroplasts or mitochondria, two possible locations for this enzyme. Our results show that targeting of FC1 to chloroplasts results in increased expression of the nuclear-encoded chloroplast genes *GUN4*, *CA1*, *HEMA1*, *LHCB2.1*, *CHLH* after treatment with Norflurazon (NF) and that this increase correlates to FC1 gene expression and haem production measured by feedback inhibition of protochlorophyllide synthesis. Targeting FC1 to mitochondria did not enhance the expression of nuclear-encoded chloroplast genes after NF treatment. The overexpression of FC1 also increased nuclear gene expression in the absence of NF treatment, demonstrating that this pathway is operational in the absence of a stress treatment. Our results therefore support the hypothesis that haem synthesis is a promotive chloroplast-to-nucleus retrograde signal. However, not all FC1 overexpression lines enhanced nuclear gene expression, suggesting there is still a lot we do not understand about the role of FC1 in this signalling pathway.

This article is part of the theme issue 'Retrograde signalling from endosymbiotic organelles'.

1. Introduction

Chloroplasts evolved through the integration of a free-living photosynthetic prokaryote into a non-photosynthetic eukaryote, followed by relocation of the majority of the chloroplast genome to the nucleus [1]. The chloroplast retains its own reduced genome, encoding less than 100 predicted proteins in *Arabidopsis thaliana*, with the remaining approximately 3000 proteins encoded in the nucleus and imported into the developing chloroplast [2]. Consequently, there is a requirement for bidirectional signalling pathways between these organelles to ensure correct provision of proteins to the chloroplast. Anterograde signalling pathways by which the nucleus controls chloroplast development are reasonably well characterized and include photoreceptor and hormone control of nuclear-encoded chloroplast proteins [1,3], some of which can control the expression of chloroplast-encoded proteins [4,5]. Signalling from the chloroplast to the nucleus during chloroplast development (termed biogenic retrograde signalling; [6]) is more poorly understood. However, treatments leading to chloroplast damage at the developmental stage result in a strong

downregulation of hundreds of nuclear-encoded genes, many encoding chloroplast proteins [7,8]. In addition, the impact of the environment on photosynthesis enables chloroplasts to fulfil a sentinel function for environmental stress, and various operational retrograde signals from mature chloroplasts can regulate nuclear gene expression to acclimate to these stresses [6,9,10].

Our understanding of biogenic retrograde signalling is based on the identification of *genomes uncoupled* (*gun*) mutants in which expression of the nuclear-encoded *LHCB1.2* gene is maintained after severe chloroplast damage that strongly inhibits expression of many nuclear-encoded photosynthetic genes [11]. In this case, chloroplast development was prevented by treatment with the phytoene desaturase inhibitor Norflurazon (NF), which blocks the production of photoprotective carotenoids [12,13]. Of the five originally described *gun* mutations, four were in genes encoding proteins required for the synthesis of tetrapyrroles. *gun2* and *gun3* are haem oxygenase and phytychromobilin synthase mutants, respectively, with reduced ability to convert haem to phytychromobilin [14]. The *gun5* mutation is in the gene encoding the H subunit of Mg-chelatase [14] and *gun4* lacks a positive regulator of Mg-chelatase [15]. Initial ideas around Mg-protoporphyrin IX (Mg-proto) functioning as a mobile retrograde signal [16] have mostly been unsupported as no correlation was observed between Mg-proto levels and *Lhcb* gene expression when Mg-proto levels were manipulated chemically [17] or genetically [18]. Instead, the identification of the dominant *gun6* mutation that results in elevated ferrochelatase (FC) 1 activity seemed to resolve the *gun* mutant puzzle and led to the hypothesis that synthesis of the FC1 product, haem, was required to promote expression of nuclear-encoded photosynthetic genes [19]. As well as making sense of the impact of the *gun* mutations on tetrapyrrole biosynthesis, this hypothesis was consistent with an established role for haem as a signalling molecule in many systems, its relative suitability in terms of its chemistry and its known export from chloroplasts [20].

The retrograde signalling field has struggled in recent years with proposed components of the signalling pathway that have not stood up to scrutiny. Recent examples of mutants for which a reported *gun* phenotype has not been reproducible in other laboratories include those lacking PTM1 [21] and ABI4 [22]. However, the phenotypes of the *gun* mutants themselves have been observed in many laboratories over a long period, including the more recently identified *gun6* mutant [21]. In the current study, we set out to test the hypothesis that FC1 overexpression results in an increase in a promotive retrograde signal, by constructing plants overexpressing FC1. In *Arabidopsis* (and other higher plants), there are two genes encoding ferrochelatase, *FC1* and *FC2*. The expression profile [17,23–25] and functional analysis [26–29] of these genes are consistent with FC1 having a role in providing non-photosynthetic haem and FC2 being required for photosynthetic haem production. For example, mutants lacking FC1 show poor early development with strong alleles being embryo lethal [28,29] and reduced accumulation of extra-plastidic cytochromes [28]. By contrast, the loss of FC2 results in poor chlorophyll accumulation and reduced development of the photosynthetic apparatus [26–28]. The *fc2* mutants also show reduced total haem levels. FC2 can partially compensate for the loss of FC1 if expressed from the *FC1* promoter [29] and FC1 (with an FC2 transit peptide) can partially compensate for the loss of FC2 [27].

There is considerable biochemical evidence that both chloroplasts and mitochondria contain ferrochelatase activity and activity of the preceding enzyme in the pathway, protoporphyrinogen IX oxidase [30–34]. Import experiments in purified organelles also demonstrated that while FC2 was restricted to chloroplasts, FC1 was imported into both chloroplasts and mitochondria, albeit with the majority of FC1 localized in the former [35,36], and recently, haemagglutinin-tagged FC1 was detected in mitochondrial fractions [34]. These data continue to suggest the possibility of the dual localization of FC1, although some studies do not support this (e.g. [37]). There are links between mitochondria and chloroplasts in retrograde signalling responses [38–40] and it is possible that FC1 may mediate its effect through mitochondrial localization. We have therefore expressed FC1 with its predicted transit peptide replaced with transit peptides specific for plastid (RecA) or mitochondrial import (CoxIV). The RecA and CoxIV transit peptides were selected as they have been used previously to successfully target proteins to these respective organelles [41–43]. Our results show that targeting of FC1 to plastids alone is sufficient to promote expression of nuclear-encoded photosynthetic genes, and thus, our data support the hypothesis that chloroplast-localized FC1 activity is required for retrograde signalling.

2. Material and methods

(a) Plant material and growth conditions

The *gun5* [14] and *gun6* [19] mutants in the Col-0 background have been described previously. For growth on plates, seeds were surface-sterilized with 70% (v/v) ethanol and 10% (v/v) bleach solutions, and plated seeds then imbibed for 3 days at 4°C in the dark. For selection of transgenics, seeds were plated onto half-strength Murashige and Skoog (MS) medium containing 1% (w/v) agar, pH 5.8, supplemented with 40 µg ml⁻¹ hygromycin B. For the growth of transgenics to determine transgene expression levels, seeds were plated onto half-strength MS medium containing 1% (w/v) agar, pH 5.8. After imbibition, seeds were transferred to WLc (100 µmol m⁻² s⁻¹) at 23°C for 5 days. For NF screens, seeds were plated onto half-strength Linsmaier and Skoog (LS) medium containing 1% (w/v) sucrose and 1% (w/v) agar, pH 5.8 and supplemented with either 5 µM NF or 0.1% DMSO (control). After imbibition, seeds were transferred to continuous low white light (LWLc; 25 µmol m⁻² s⁻¹) at 23°C for 7 days. For growth in soil, seeds were sown directly onto compost (Levington's F2 : John Innes No. 2 : vermiculite; 1 : 1 : 1) and grown in photoperiods of 16 h white light, 8 h dark at 23°C with a relative humidity of 65%.

(b) Generation of transgenic *Arabidopsis thaliana* lines

The coding sequence of *FC1* was fused at the 3' end to a solubility-modified, red-shifted *GFP* [43], hereafter referred to as *GFP*. A 36 bp spacer was present between the *FC1* sequence and the *GFP* sequence. In addition, the native transit peptide of FC1 was excluded. This was identified from predictions made using TargetP 1.1 Server [44,45], predictions of the target peptide cleavage sites based on known cleavage sequences and alignment of protein sequences to identify amino acids required for function that are conserved across other plant and cyanobacterial species. Following this analysis, the sequence encoding the first 77 amino acids of FC1 (*FC1A*^{1–77}) was excluded. A BglIII restriction site was added 5' of the *FC1A*^{1–77}:*GFP* sequence. The *FC1*:*GFP* fragment was cloned into pDONR1M221 (Invitrogen, Carlsbad, CA, USA) using Gateway[®] technology. A transit peptide conferring

localization either to plastids (*RecA*) or mitochondria (*CoxIV*) was then ligated directly upstream of the gene sequence (at the BglIII site) to generate the expression cassettes. The *RecA* transit peptide sequence corresponded to the first 201 bp of the coding sequence of the Arabidopsis *RECA* gene (At1g79050; [46]), while the *CoxIV* transit peptide corresponded to the first 87 bp of the coding sequence of cytochrome *c* oxidase subunit 4 from *Saccharomyces cerevisiae* [47]. Control expression cassettes lacking *FC1* were also created, consisting of the *GFP* sequence fused downstream of the *RecA* or *CoxIV* transit peptide sequences. Finally, a cassette consisting of the full-length *FC1* (FL-*FC1*) sequence fused to *GFP* was created. The cassettes were recombined into the pGWB502 Ω (*hyg*^R) plant expression plasmid [48] under the control of the 35S promoter from cauliflower mosaic virus, and the resulting plasmids were used to transform *Agrobacterium tumefaciens* GV3101. Flowering Arabidopsis Col-0 plants were transformed using the floral dip method [49], and positive transformants identified through antibiotic selection [50] were confirmed *via* PCR genotyping. Further details on the primers and plasmids used are given in electronic supplementary material, tables S1 and S2, respectively. Plants overexpressing *FC1* targeted to both plastids and mitochondria were generated by manually crossing *CoxIV:FC1:GFP* lines (female) to *RecA:FC1:GFP* lines (male).

(c) RNA extraction, cDNA synthesis and qRT-PCR

Cotyledon tissue was homogenized in 500 μ l extraction buffer (100 mM NaCl, 10 mM Tris pH 7.0, 1 mM EDTA, 1% (w/v) SDS). After the addition of 150 μ l phenol (pH 4.8), samples were vortexed vigorously. After the addition of 150 μ l phenol (pH 4.8), samples were vortexed vigorously. This was followed by the addition of 250 μ l chloroform and the samples were again vortexed vigorously. After centrifugation (16 100g, 5 min, 4°C), the upper aqueous phase was transferred to a new tube containing 450 μ l ice-cold 4 M LiCl. RNA was precipitated overnight at 4°C. After centrifugation (16 100g, 20 min, 4°C), pellets were resuspended in 300 μ l DNase buffer (10 mM Tris pH 7.5, 2.5 mM MgCl₂, 0.5 mM CaCl₂). One microlitre DNase (Promega, Madison, WI, USA) was then added and samples incubated at 37°C for 25 min. Samples were mixed with 500 μ l phenol:chloroform:isoamyl alcohol (25:24:1), pH 6.7 and vortexed vigorously. After centrifugation (16 100g, 5 min, 4°C), the aqueous upper phase was mixed with 750 μ l 95% ethanol:5% 3 M sodium acetate, pH 5.2 and RNA was precipitated at -20°C for 1 h. After centrifugation (16 100g, 20 min, 4°C), RNA pellets were air-dried and resuspended in 50 μ l TE buffer (10 mM Tris pH 8.0, 1 mM EDTA).

cDNA synthesis was performed according to the manufacturer's protocols on 2 μ g total RNA per sample with the nanoScript2 kit (Primerdesign, Southampton, UK), using random nonamer and oligo dT primers.

qRT-PCR was carried out on a StepOnePlus™ real-time PCR system (Applied Biosystems, Foster City, CA, USA). Each reaction contained 0.5 μ l cDNA, 5 μ l PrecisionPLUS SYBR green mastermix (Primerdesign) and 2.5 μ l of primer mix (containing forward and reverse primers each at 2 μ M), with the volume made up to 10 μ l with nuclease-free water. qRT-PCR primer sequences are given in electronic supplementary material, table S3. Two technical replicates were performed for each sample/primer pair combination, and two 'no template controls' were performed for each primer pair. qRT-PCR cycling conditions were: 95°C for 2 min, followed by 40 cycles of 95°C for 15 s and 60°C for 1 min, with fluorescence determined at the end of every cycle. Melt curves (60°C to 92°C, in 0.5°C increments) were performed at the end of every run to verify amplification specificity for each primer pair. Primer efficiencies were determined using a serial dilution of Col-0 (untreated) cDNA. Relative expression values between samples were calculated using the $\Delta\Delta$ Ct method, normalized to *ACTIN DEPOLYMERISING FACTOR 2* (*ADF2*, At3g46000) or *YELLOW-LEAF-SPECIFIC GENE 8* (*YLS8*, At5g08290). *ADF2* and *YLS8*

were identified as excellent reference genes for NF screens through analysis of microarray data from Col-0 seedlings grown with/without NF [51]. Data shown were normalized to *ADF2*, with comparable results observed when normalized to *YLS8*. Full details of the qRT-PCR method to fulfil MIQE guidelines [52] are given in electronic supplementary material, datasheet S1.

(d) Chlorophyll, carotenoid and Pchlde determination

Chlorophyll and carotenoids were extracted from weighed cotyledon tissue by homogenizing in 800 μ l ice-cold 80% (v/v) acetone. After centrifugation (16 100g, 5 min, 4°C), the absorbance of the supernatant was determined at A_{470} , A_{647} and A_{663} using a U-2001 spectrophotometer (Hitachi, Tokyo, Japan). Total carotenoid and chlorophyll *a* and *b* contents were determined using previously published equations [53], and normalized to tissue weight.

Pchlde was extracted from cotyledon tissue harvested in a dark room under a dim green safe light using the method described in Terry & Kaprzak [54]. Cotyledon pairs were homogenized in ice-cold acetone:0.1 M ammonium hydroxide (9:1, v:v), centrifuged (16 100g, 5 min, 4°C), and fluorescence emission spectra of the supernatants determined (excitation wavelength = 440 nm) using a F-2000 fluorescence spectrophotometer (Hitachi, Tokyo, Japan). The height of the Pchlde peak (~636 nm) was used to generate relative fluorescence values, which were normalized for cotyledon number.

(e) Localization of GFP by confocal imaging

Confocal imaging was used to confirm the subcellular localization of plastid- and mitochondrion-targeted *FC1*. Cotyledon tissue from 5 day continuous white light (WLC)-grown seedlings was mounted onto slides and the samples were flooded with the perfluorocarbon PP11. The localization of GFP was determined on a Leica TCS SP8 confocal microscope (Leica Microsystems, Wetzlar, Germany), using Leica Application Suite X software. GFP was imaged with an excitation wavelength of 488 nm and detection of emission between 497 and 531 nm, both using the 63 \times glycerol oil immersion objective lens. Chlorophyll autofluorescence was detected using 488 nm excitation and 678–695 nm emission. An HyD detector was used to image both signals, and at least six averages were taken for each acquisition.

3. Results

(a) Characterization of *FC1* overexpressing lines

We generated transgenic lines containing either a *RecA:FC1:GFP* (plastid-targeted, pFC1) or a *CoxIV:FC1:GFP* (mitochondrion-targeted, mFC1) expression cassette driven by the constitutive CaMV 35S promoter. Selection protocols were used to identify single-insertion, homozygous transformants (T_3 generation) and, subsequently, overexpressing lines were determined by measuring the *FC1* expression level in cotyledon tissue from 5-day-old WLC-grown seedlings using qRT-PCR. For the pFC1 lines, expression ranged from 2- to 85-fold higher than wild-type (WT, Col-0) under these conditions (figure 1a). *FC1* expression levels correlated with *GFP* expression levels from the same plants, while *FC2* expression remained essentially at a WT level (electronic supplementary material, figure S1a). Some of these lines displayed a pale cotyledon phenotype that appeared to correlate with *FC1* expression, with high overexpressors having very pale cotyledons and low overexpressors being indistinguishable from WT (electronic supplementary material, figure S2a). Control lines overexpressing only *GFP* targeted to plastids lacked a visible phenotype (electronic

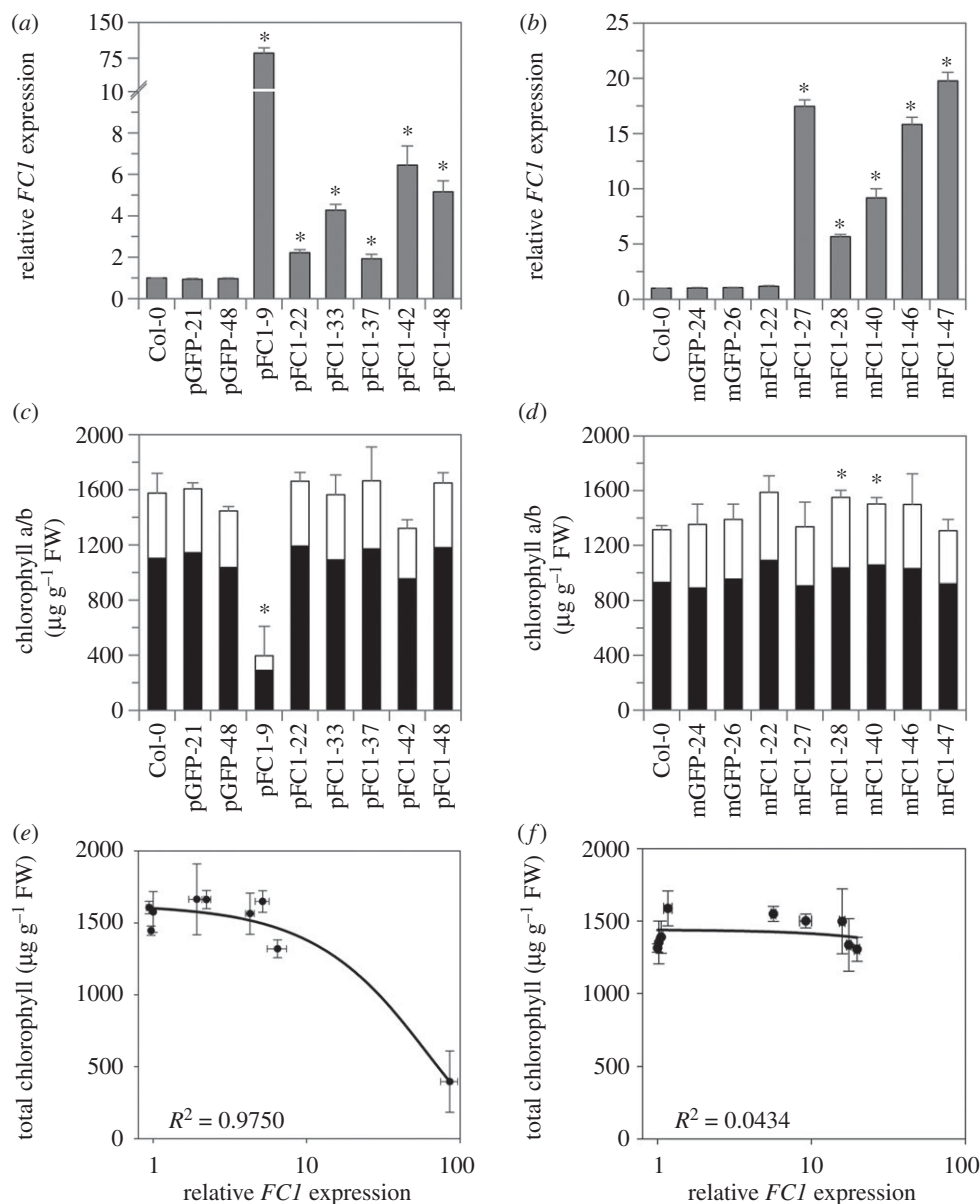


Figure 1. The relationship between *FC1* expression and chlorophyll content in the pFC1 and mFC1 transgenic lines. (a,b) *FC1* expression relative to Col-0 in (a) plastid-targeted (pFC1) and (b) mitochondria-targeted (mFC1) *FC1* overexpressing lines as determined by qRT-PCR. (c,d) Total chlorophyll content of the same pFC1 (c) and mFC1 (d) lines. Black bars represent chlorophyll *a* and white bars represent chlorophyll *b*. (e,f) Correlation plots between *FC1* expression (log scale) and total chlorophyll content for the pFC1 (e) and mFC1 (f) lines. Seedlings were grown for 5 days in WLC for all analyses and lines overexpressing only *GFP* in plastids (pGFP) or mitochondria (mGFP) were included as controls. Data represent the mean + s.e.m. of three independent biological replicates and asterisks indicate a significant difference versus Col-0 ($p < 0.05$, Student's *t*-test).

supplementary material, figures S1a and S2a). The correlation between the pale cotyledon phenotype and *FC1* expression level was confirmed by analysis of the chlorophyll content of these lines when grown under the same conditions, with the highest overexpressor (pFC1-9) having significantly less total chlorophyll than WT (figure 1c,e). The pFC1-9 line also had significantly less total carotenoids than WT (electronic supplementary material, figure S2b). The next highest overexpressor (pFC1-42) also indicated reductions in chlorophyll and carotenoid content, although these were not statistically significant (figure 1c; electronic supplementary material, figure S2b). *FC1* overexpressing lines using the native transit peptide have previously been reported to have a reduction in chlorophyll synthesis [19]. The chlorophyll *a/b* ratio of all pFC1 lines remained similar to WT (electronic supplementary material, figure S2c) and there was no significant effect of day length or light intensity on the accumulation of chlorophyll or

carotenoids in these lines (electronic supplementary material, figure S3). Surprisingly, the pale phenotype of pFC1-9 was partially attenuated in mature, soil-grown plants, while the pFC1-42 line showed a paler phenotype compared to seedlings (electronic supplementary material, figure S4).

For the mFC1 lines, *FC1* expression in 5-day-old WLC-grown seedlings ranged from 1.2- to 20-fold higher than WT (figure 1b). *GFP* expression again correlated with *FC1* expression, with *FC2* expression fundamentally unaffected (electronic supplementary material, figure S1b). No phenotypic differences from WT were observed in these lines at any stage of growth (figure 1d,f; electronic supplementary material, figures S4-S6).

Although the paler phenotype of the two transgenic lines pFC1-9 and pFC1-42 correlated quite well with *FC1* expression levels, we wanted to be certain that the observed phenotypes were not owing to the insertion site of the *FC1* transgene. We therefore performed whole-genome sequencing on both lines

to identify the location of the transgenes. As shown in electronic supplementary material, figure S7, the *RecA-FC1-GFP* transgene in pFC1-9 has interrupted the 3' end of At1g01540 at the end of exon 6. All sequence reads indicate that insertion has occurred solely at one location in the genome and confirm our original results from antibiotic selection of T2 seed. At1g01540 is a protein related to Thylakoid-associated kinase 1, but has been determined experimentally to be a cytosolic protein [55]. A GABI-Kat mutant was reported as showing no obvious phenotype [56] and we also obtained independent T-DNA insertion lines for At1g01540 (Salk_008396, Salk_076898 and Salk_036951), but could see no visible loss of greening phenotype at the seedling stage. For pFC1-42, there was a single-insertion site in an intergenic region in chromosome 5 that lies about 600 bp upstream of the start codon of At5g67120 and about 1250 bp upstream of the start codon of At5g67130. There appear to be up to four T-DNA copies at this single-insertion site. At5g67120 and At5g67130 encode an uncharacterized RING/U-box superfamily protein predicted to be nuclear-localized and a plasma membrane-localized [57] phospholipase C-like phosphodiesterase superfamily protein with phospholipase activity [58], respectively. It is possible that the T-DNA insertion could interfere with the expression of either or both genes, but there is no evidence to suggest that this might cause the pFC1-42 phenotype.

(b) Localization of FC1-GFP proteins

To confirm the localization of the plastid and mitochondrion-targeted GFP fusion proteins, we examined 5-day-old WLc-grown seedlings using confocal imaging. GFP localization was performed on root tips and cotyledons of the highest over-expressing pFC1 and mFC1 lines. When imaging root tips, GFP-labelled structures in cells of pFC1 seedlings were significantly larger than those in mFC1 seedlings (Student's *t*-test $p < 0.001$, figure 2*a,b*). Moreover, the sizes of the structures in the pFC1 and mFC1 lines closely matched the known sizes of root plastids and mitochondria, respectively (pFC1 = $5.70 \mu\text{m} \pm 0.08$, mFC1 = $1.63 \mu\text{m} \pm 0.12$) [59]. In addition, the GFP-labelled structures in the mFC1 lines moved rapidly during imaging, supporting the identification of these structures as mitochondria. For lines pFC1-9 and pFC1-42, imaged cotyledons were pale with very few chlorophyll-containing cells (figure 2*a*). GFP was detected in plastids lacking chlorophyll, while no GFP signal was observed when chlorophyll was present. This suggests that the ability to synthesize chlorophyll is an inverse function of plastid *FC1* expression such that high expression of *FC1* protein necessarily limits chlorophyll accumulation. The imaging of mFC1-27 cotyledons further supported mitochondrial localization of *FC1* in these lines, given the absence of overlap and difference in size between the GFP-labelled structures in this line and chloroplasts (figure 2*b*). As expected, a control line in which *GFP* was overexpressed in the absence of a transit peptide showed cytosolic localization (figure 2*c*).

(c) Retrograde signalling in FC1 overexpressing lines

It was previously demonstrated that the overexpression of full-length *FC1* with its native transit peptide rescued the expression of photosynthesis-associated nuclear genes when seedlings were grown on NF (*gun* phenotype) [19]. To establish whether organellar-specific overexpression of *FC1* was sufficient to replicate the *gun* phenotype, the transgenic lines

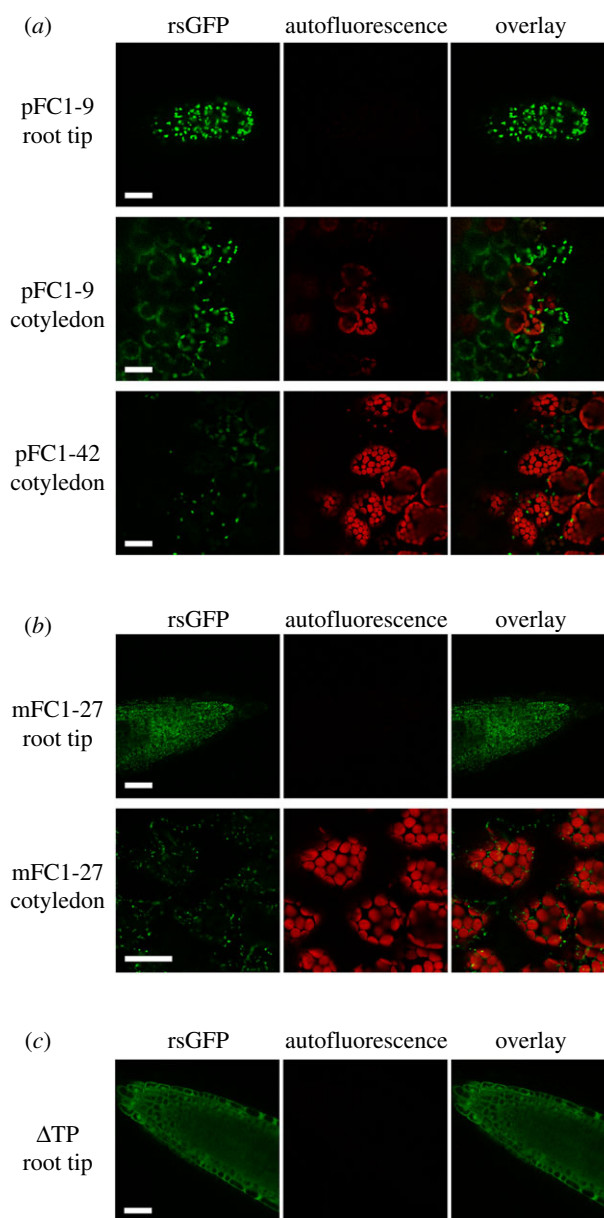


Figure 2. Localization of *FC1* in roots and cotyledons of pFC1 and mFC1 seedlings. (*a,b*) Confocal microscopy was used to determine the subcellular localization of *FC1*:GFP fusion proteins in pFC1 (*a*) and mFC1 (*b*) lines. (*c*) A control line of *FC1*:GFP without a transit peptide (Δ TP). Scale bars, 30 μm .

described above were grown on NF and expression of nuclear genes determined. *gun5* and *gun6* were included in these screens as positive controls and lines overexpressing *GFP* alone in either plastids (pGFP) or mitochondria (mGFP) were included as negative controls. In the presence of NF, the two highest expressors of plastid-targeted *FC1* (pFC1-9 and pFC1-42) were able to significantly rescue expression of all five nuclear genes tested (*GUN4*, *CA1*, *HEMA1*, *LHCB2.1* and *CHLH*), when compared with Col-0 and pGFP seedlings (figure 3*a*; electronic supplementary material, figure S8*a*). By contrast, the highest overexpressing mFC1 lines were not able to rescue the expression of any of the genes tested (figure 3*b*; electronic supplementary material, figure S8*b*). Importantly, growth on NF did not have a strong effect on the expression of *FC1* in the lines tested (electronic supplementary material, figure S9) and results were independent of the reference gene used (electronic supplementary material, figure S10). Correlation plots of percentage recovery of nuclear

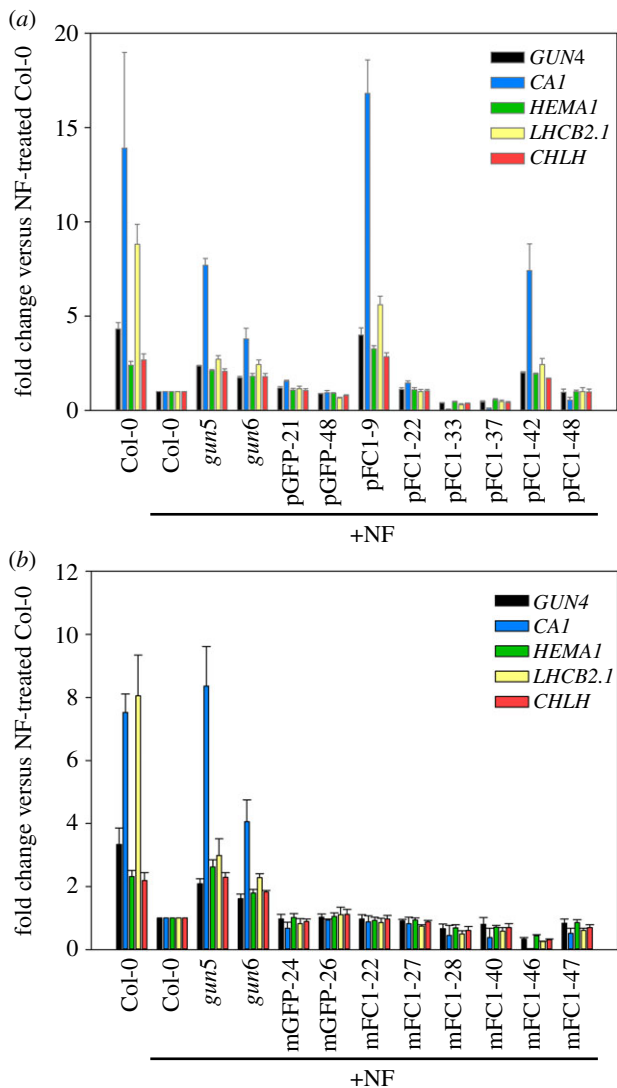


Figure 3. Expression of photosynthesis-associated genes on NF is enhanced in plastid *FC1*, but not mitochondrial *FC1* overexpressors. (a,b) The expression of *GUN4*, *CA1*, *HEMA1*, *LHC2.1* and *CHLH* was determined by qRT-PCR in pFC1 (a) and mFC1 (b) seedlings grown for 7 days in LWLC on plates with NF. The control lines pGFP (a) and mGFP (b), as well as *gun5* and *gun6*, were included. Data shown are the mean fold changes versus Col-0 on NF + s.e.m. of three independent biological replicates. The original qRT-PCR data for these graphs are given in electronic supplementary material, figure S8.

gene expression (for all five genes pooled together) after NF treatment versus WT and *FC1* expression in the presence of NF show a positive correlation for the plastid-targeted overexpressors (figure 4a), but no correlation for the mitochondrion-targeted overexpressors (electronic supplementary material, figure S11a). These results strongly support the idea that the overexpression of *FC1* targeted to plastids is sufficient to rescue expression of nuclear-encoded photosynthesis genes in the presence of NF. Interestingly, both pFC1 and mFC1 lines showed a positive correlation between percentage change in nuclear gene expression and *FC1* expression in the absence of NF (figure 4b; electronic supplementary material, figure S11b), although the maximum increase in expression was just 10% for mFC1 lines compared to 50% for pFC1 lines. The increase in nuclear gene expression observed in pFC1 lines demonstrates the operation of this retrograde pathway under standard plant growth conditions.

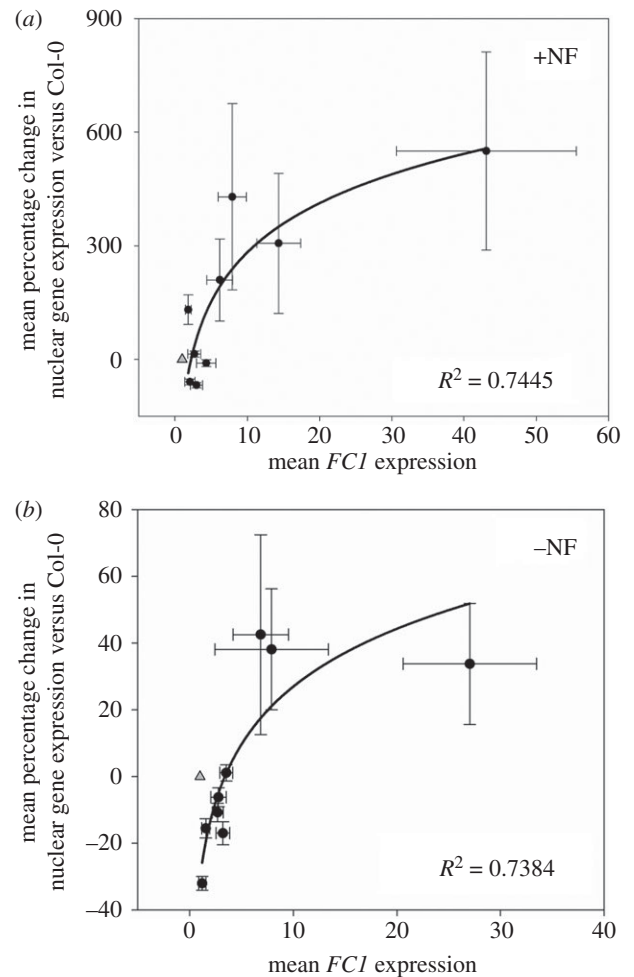


Figure 4. Plastid-targeted *FC1* expression correlates with enhanced nuclear gene expression on NF. (a,b) Correlation plots of the combined mean percentage change in expression of *GUN4*, *CA1*, *HEMA1*, *LHC2.1* and *CHLH*, versus *FC1* expression for pFC1 seedlings in the presence (a) or absence (b) of NF. Data are relative to Col-0 +NF (a) or –NF (b). For both graphs, data points include *gun6*, the six transgenic pFC1 overexpressing lines and two F1 progenies of pFC1x mFC1 crosses. The triangles indicate WT response. SigmaPlot 13.0 was used to fit logarithmic best-fit lines and derive coefficients of determination. Data shown are the mean ± s.e.m. of three independent biological replicates.

Next, we tested whether the effect of elevated plastid *FC1* expression on nuclear gene expression required photoreceptor input in order to be observed. We therefore tested the same five nuclear genes (*GUN4*, *CA1*, *HEMA1*, *LHC2.1* and *CHLH*) in seedlings grown for 4 days in the dark. In this case, we saw little difference in expression between pFC1 or mFC1 lines and WT for any genes tested (electronic supplementary material, figure S12), except for *HEMA1* expression, which was slightly, yet significantly, increased in pFC1–9 in the dark compared to Col-0 (electronic supplementary material, figure S12a). An increase in *HEMA1* expression in dark-grown seedlings has previously been noted for *gun1* seedlings [60].

To determine if overexpression of *FC1* in both organelles would modify the rescue of nuclear gene expression on NF seen in pFC1 lines, pFC1–9 (the highest expressor of plastid-targeted *FC1*) was independently crossed with both mFC1–27 and mFC1–47 (the two highest mitochondrion-targeted *FC1* overexpressors), and the F₁ generation screened on NF. The three parent lines were included in the screens for reference.

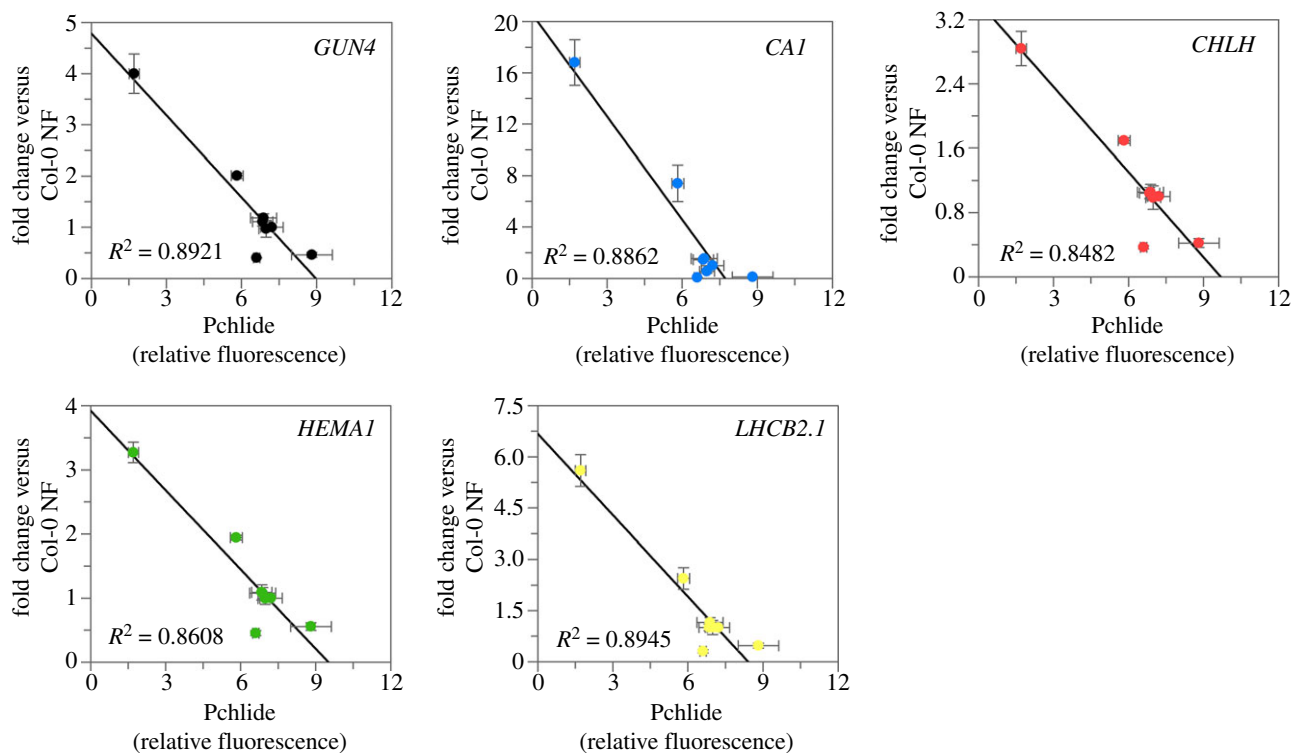


Figure 5. Enhancement of nuclear gene expression on NF inversely correlates with protochlorophyllide levels in dark-grown pFC1 seedlings. Correlation plots of protochlorophyllide (Pchlde) in 4-day-old dark-grown pFC1 seedlings against fold change in expression of *GUN4*, *CA1*, *HEMA1*, *LHC2.1* and *CHLH* versus Col-0 on NF. Data represent the mean \pm s.e.m. of three independent biological replicates.

F₁ plants of both the mFC1-47 \times pFC1-9 and mFC1-27 \times pFC1-9 lines showed significant enhancement of gene expression after NF treatment (see *CA1* and the tetrapyrrole biosynthesis genes; electronic supplementary material, figure S13*a*), but expression levels were reduced compared with the pFC1-9 parent line. This was most likely owing to the greatly reduced *FC1* expression levels in the F₁ plants compared to the parent lines (electronic supplementary material, figure S13*b*). The observation that F₁ generation FC1 overexpressing plants can confer a *gun* phenotype demonstrates that this trait is semi-dominant and provides further evidence that the observed phenotype is solely the result of FC1 overexpression.

(d) Modulation of tetrapyrrole synthesis in FC1 overexpressing seedlings correlates with induction of nuclear gene expression

Lines overexpressing plastid-localized *FC1* were able to enhance nuclear gene expression on NF, and this ability correlated with *FC1* expression. To determine if this enhancement of gene expression was owing to changes in haem synthesis as proposed by the current model [19,20], we examined the impact of the overexpressing lines on tetrapyrrole synthesis and determined whether this was also correlated with nuclear gene expression. As it is difficult to measure a signalling haem pool in young seedlings, we determined the accumulation of protochlorophyllide (Pchlde) in the dark as a proxy for such a haem pool at the onset of the light treatment. It is well established that the accumulation of haem results in feedback inhibition of aminolevulinic acid (ALA) synthesis resulting in reduced Pchlde [61–64]. Previous studies have observed elevated Pchlde in *fc2* mutants,

but not *fc1* mutants, suggesting that FC2-synthesized haem is responsible for feedback inhibition [26]. However, it has been shown that overexpression of FC1 can rescue this phenotype [27], indicating that FC1-synthesized haem can contribute to this regulatory pool. In pFC1 seedlings, Pchlde accumulation in the dark (electronic supplementary material, figure S14) showed a strong negative correlation with expression of all five nuclear genes on NF (figure 5). This correlation was not apparent for mFC1 seedlings (electronic supplementary material, figure S15). Together, these data suggest that there is an elevated regulatory haem pool in pFC1 lines that correlates well with the observed increases in nuclear gene expression in these lines. These results therefore support the hypothesis that increased FC1 activity results in the production of a promotive retrograde signal [19] and, furthermore, that activity in the plastid alone is sufficient for this response.

4. Discussion

The interpretation of the *gun* mutant phenotype has been the focus of our attempts to understand chloroplast-to-nucleus retrograde signalling since these mutants were first described over 25 years ago [11]. Five of the six *gun* mutants isolated by the Chory laboratory had altered activities of tetrapyrrole biosynthesis-related proteins [14,15,19] and the link between tetrapyrrole synthesis and retrograde signalling has stood up to scrutiny over this period. The current hypothesis is that haem synthesized by FC1 is a promotive retrograde signal or precursor of the signal ([19]; see [20,65,66] for discussion). This hypothesis is based on the observation that both the dominant *gun6* mutation that results in overexpression of *FC1* and a

transgenic FC1 overexpression line resulted in enhanced nuclear gene expression after NF treatment and was developed through the re-interpretation of the phenotypes of the *gun2–gun5* mutants [19]. Consistent with this hypothesis, haem has a well-established role as a mobile signalling molecule in numerous biological systems [20]. Here, we have shown that overexpression of FC1 in chloroplasts results in a strong *gun* phenotype in two independent transgenic lines and that expression of five nuclear-encoded photosynthetic genes correlated with FC1 gene expression and the ability to feedback inhibit Pchlide synthesis. Our data therefore broadly support the hypothesis that FC1-dependent haem synthesis results in a promotive chloroplast-to-nucleus retrograde signal. Moreover, this signal is directly related to FC1 activity in the chloroplast as no evidence was observed for a *gun* phenotype when FC1 was targeted to mitochondria. This result is consistent with previous experiments in which overexpression of FC1 using an FC2 transit peptide could increase nuclear gene expression after NF treatment [19], although formally the localization of the FC2-targeted FC1 protein *in vivo* is unknown as GFP-tagged FC proteins have never been detected in mitochondria, despite the strong evidence for the presence of FC in this organelle. Although we were unable to isolate a very highly expressing mFC1 line to match the level of FC1 overexpression seen in line pFC1–9, under the conditions of the NF screen, three of the mFC1 lines had clearly higher FC1 expression than pFC1–42, a line that shows significant rescue of nuclear gene expression on NF. Our data do not therefore support a model in which a chloroplast retrograde signal could have made use of presumably pre-existing mitochondrial signals. Instead, there appears to be direct regulation of nuclear-encoded genes for chloroplast proteins during chloroplast biogenesis.

During the course of this study, we identified six lines that showed elevated expression of FC1 in cotyledon tissue under the conditions used for the retrograde signalling assays. Only two of these lines showed a *gun* phenotype, but we included data for all six lines as we wanted to be transparent about the issues we encountered. For example, three of the pFC1 lines (pFC1–22, pFC1–33 and pFC1–48) had similar or higher levels of FC1 expression on NF than the *gun6* mutant but did not show a *gun* phenotype, and the pFC1–42 and pFC1–48 lines had similarly high FC1 expression but showed different gene expression responses. This discussion is complicated by the observation that FC1 expression in *gun6* decreases on NF, something not observed in the overexpression lines. Only pFC1–9 and pFC1–42 showed higher FC1 expression than *gun6* in the absence of NF and this may account for their ability to confer a *gun* phenotype while other lines were unable to. Importantly perhaps, only these two lines had expression levels that were sufficient to impact on chlorophyll accumulation. Woodson *et al.* [19] reported reduced chlorophyll levels in all lines that also showed a *gun* phenotype. We are confident that the phenotypes we observed are owing to FC1 overexpression. Genome sequencing to identify the position of each overexpression construct ruled out the likelihood of an insertional effect causing the observed phenotype and the pFC1–9 construct showed a semi-dominant phenotype following crosses with mFC1 lines. Interestingly, even the pFC1–9 and pFC1–42 lines showed slightly different phenotypes, with the former showing a stronger reduction in chlorophyll levels in seedlings and the latter having a more pronounced mature plant phenotype. This might be related to positional

effects altering expression levels in different tissues. Overall, a far more detailed characterization of FC1 protein levels, localization and activity as well as haem levels for each line would be required to explain the observed phenotypic differences between the different FC1 overexpressing lines. Nevertheless, we believe that our observation that overexpression of FC1 in chloroplasts can confer a *gun* phenotype, which confirms and builds on the results of Woodson *et al.* [19], is important in helping to establish an agreed set of reliable data on the retrograde signalling response.

One interesting aspect of our data is the clear demonstration that overexpression of FC1 resulted in an increase in nuclear gene expression in the absence of NF treatment. Expression of key genes increased up to 50% in pFC1 lines. A small increase was also observed in mFC1 lines, although this was not significant for any individual line (electronic supplementary material, figure S8). One of the criticisms of the retrograde signalling field is the perceived requirement for severe treatments to observe the effects of mutations that affect signalling. Our data therefore support the idea that retrograde signalling is functioning under standard growth conditions and that the amount of signal is not necessarily limited. This result therefore supports previous data such as elevated *HEMA1* expression in a *gun1, gun5* double mutant during de-etiolation [60].

Finally, a central question in retrograde signalling research is whether single or multiple signals are operating during chloroplast biogenesis. The question derives from analysis of the *gun1* mutation that confers elevated nuclear gene expression after treatments with either NF or the plastid translation inhibitor, lincomycin [7], which has led to the suggestion that GUN1 mediates a signal related to plastid protein synthesis. Indeed, GUN1 does seem to have a role in plastid protein homeostasis [67–69]. However, recently, other roles have also been suggested in chloroplast RNA editing [70] and import of nuclear-encoded chloroplast proteins [71]. GUN1 has also been shown to interact with tetrapyrrole biosynthesis enzymes [67] and to bind haem and a range of porphyrins and regulate FC1 enzyme activity *in vitro* [72]. Given the strong evidence for a tetrapyrrole signal from the haem branch of the pathway, it could be proposed that GUN1 might have a role in coordinating various chloroplast processes with production of the FC1-dependent haem signal. Certainly, an understanding of the relationship between GUN1 and FC1-mediated retrograde signalling will be crucial in determining the mechanism of this signalling pathway during chloroplast development.

Data accessibility. All datasets supporting this article have been provided as part of the electronic supplementary material.

Authors' contributions. M.T.P. performed all of the experiments and analysed data; T.G-B. contributed to making the FC1 overexpressing lines; A.S. conceived the project and analysed data. M.J.T. conceived the project and analysed data. All authors contributed to writing the article and approved the final version.

Competing interests. We have no competing interests.

Funding. M.T.P., T.G-B. and M.J.T. were supported by UK Biotechnology and Biological Sciences Research Council (BBSRC) grant no. BB/J018139/1. A.G.S. was supported by BBSRC grant no. BB/J018694/1.

Acknowledgements. Thanks to Joanne Chory and Jesse Woodson (SALK Institute, USA) for the *gun5* and *gun6* mutants used in this study. Thanks also to George Littlejohn (University of Exeter, UK) for the gift of PP11 and to Chiara Perico and Imogen Sparkes (University of Exeter, UK) for looking at FC1 localization in some of our transgenic lines.

- Jarvis P, López-Juez E. 2013 Biogenesis and homeostasis of chloroplasts and other plastids. *Nat. Rev. Mol. Cell Biol.* **14**, 787–802. (doi:10.1038/nrm3702)
- Abdallah F, Salamini F, Leister D. 2000 A prediction of the size and evolutionary origin of the proteome of chloroplasts of *Arabidopsis*. *Trends Plant Sci.* **5**, 141–142. (doi:10.1016/s1360-1385(00)01574-0)
- Pogson BJ, Ganguly D, Albrecht-Borth V. 2015 Insights into chloroplast biogenesis and development. *Biochim. Biophys. Acta* **1847**, 1017–1024. (doi:10.1016/j.bbabi.2015.02.003)
- Belbin FE, Noordally ZB, Wetherill SJ, Atkins KA, Franklin KA, Dodd AN. 2017 Integration of light and circadian signals that regulate chloroplast transcription by a nuclear-encoded sigma factor. *New Phytol.* **213**, 727–738. (doi:10.1111/nph.14176)
- Yoo CY, Pasorek EK, Wang H, Cao J, Blaha GM, Weigel D, Chen M. 2019 Phytochrome activates the plastid-encoded RNA polymerase for chloroplast biogenesis via nucleus-to-plastid signaling. *Nat. Commun.* **10**, 2629. (doi:10.1038/s41467-019-10518-0)
- Pogson BJ, Woo NS, Förster B, Small ID. 2008 Plastid signalling to the nucleus and beyond. *Trends Plant Sci.* **13**, 602–609. (doi:10.1016/j.tplants.2008.08.008)
- Koussevitzky S, Nott A, Mockler TC, Hong F, Sackett-Martins G, Surpin M, Lim J, Mittler R, Chory J. 2007 Signals from chloroplasts converge to regulate nuclear gene expression. *Science* **316**, 715–719. (doi:10.1126/science.1140516)
- Woodson JD, Perez-Ruiz JM, Schmitz RJ, Ecker JR, Chory J. 2013 Sigma factor-mediated plastid retrograde signals control nuclear gene expression. *Plant J.* **73**, 1–13. (doi:10.1111/tpj.12011)
- Chan KX, Phua SY, Crisp P, McQuinn R, Pogson BJ. 2016 Learning the languages of the chloroplast: retrograde signaling and beyond. *Annu. Rev. Plant Biol.* **67**, 25–53. (doi:10.1146/annurev-arplant-043015-111854)
- de Souza A, Wang JZ, Dehesh K. 2017 Retrograde signals: integrators of interorganellar communication and orchestrators of plant development. *Annu. Rev. Plant Biol.* **68**, 85–108. (doi:10.1146/annurev-arplant-042916-041007)
- Susek RE, Ausubel FM, Chory J. 1993 Signal transduction mutants of *Arabidopsis* uncouple nuclear *CAB* and *RBCS* gene expression from chloroplast development. *Cell* **74**, 787–799. (doi:10.1016/0092-8674(93)90459-4)
- Breitenbach J, Zhu C, Sandmann G. 2001 Bleaching herbicide norflurazon inhibits phytoene desaturase by competition with the cofactors. *J. Agric. Food Chem.* **49**, 5270–5272. (doi:10.1021/jf0106751)
- Oelmüller R, Levitan I, Bergfeld R, Rajasekhar VK, Mohr H. 1986 Expression of nuclear genes as affected by treatments acting on the plastids. *Planta* **168**, 482–492. (doi:10.1007/BF00392267)
- Mochizuki N, Brusslan JA, Larkin R, Nagatani A, Chory J. 2001 *Arabidopsis* genomes uncoupled 5 (*GUN5*) mutant reveals the involvement of Mg-chelatase H subunit in plastid-to-nucleus signal transduction. *Proc. Natl Acad. Sci. USA* **98**, 2053–2058. (doi:10.1073/pnas.98.4.2053)
- Larkin RM, Alonso JM, Ecker JR, Chory J. 2003 *GUN4*, a regulator of chlorophyll synthesis and intracellular signaling. *Science* **299**, 902–906. (doi:10.1126/science.1079978)
- Strand Å, Asami T, Alonso J, Ecker JR, Chory J. 2003 Chloroplast to nucleus communication triggered by accumulation of Mg-protoporphyrin IX. *Nature* **421**, 79–83. (doi:10.1038/nature01204)
- Moulin M, McCormac AC, Terry MJ, Smith AG. 2008 Tetrapyrrole profiling in *Arabidopsis* seedlings reveals that retrograde plastid nuclear signaling is not due to Mg-protoporphyrin IX accumulation. *Proc. Natl Acad. Sci. USA* **105**, 15 178–15 183. (doi:10.1073/pnas.0803054105)
- Mochizuki N, Tanaka R, Tanaka A, Masuda T, Nagatani A. 2008 The steady-state level of Mg-protoporphyrin IX is not a determinant of plastid-to-nucleus signaling in *Arabidopsis*. *Proc. Natl Acad. Sci. USA* **105**, 15 184–15 189. (doi:10.1073/pnas.0803245105)
- Woodson JD, Perez-Ruiz JM, Chory J. 2011 Heme synthesis by plastid ferrochelatase I regulates nuclear gene expression in plants. *Curr. Biol.* **21**, 897–903. (doi:10.1016/j.cub.2011.04.004)
- Terry MJ, Smith AG. 2013 A model for tetrapyrrole synthesis as the primary mechanism for plastid-to-nucleus signaling during chloroplast biogenesis. *Front. Plant Sci.* **4**, 14. (doi:10.3389/fpls.2013.00014)
- Page MT, Kacprzak SM, Mochizuki N, Okamoto H, Smith AG, Terry MJ. 2017 Seedlings lacking the PTM protein do not show a *genomes uncoupled (gun)* mutant phenotype. *Plant Physiol.* **174**, 21–26. (doi:10.1104/pp.16.01930)
- Kacprzak SM, Mochizuki N, Naranjo B, Xu D, Leister D, Kleine T, Okamoto H, Terry MJ. 2019 Plastid-to-nucleus retrograde signalling during chloroplast biogenesis does not require *ABI4*. *Plant Physiol.* **179**, 18–23. (doi:10.1104/pp.18.01047)
- Chow KS, Singh DP, Walker AR, Smith AG. 1998 Two different genes encode ferrochelatase in *Arabidopsis*: mapping, expression and subcellular targeting of the precursor proteins. *Plant J.* **15**, 531–541. (doi:10.1046/j.1365-313X.1998.00235.x)
- Singh DP, Cornah JE, Hadingham S, Smith AG. 2002 Expression analysis of the two ferrochelatase genes in *Arabidopsis* in different tissues and under stress conditions reveals their different roles in haem biosynthesis. *Plant Mol. Biol.* **50**, 773–788. (doi:10.1023/A:1019959224271)
- Nagai S, Koide M, Takahashi S, Kikuta A, Aono M, Sasaki-Sekimoto Y, Ohta H, Takamiya K-I, Masuda T. 2007 Induction of isoforms of tetrapyrrole biosynthetic enzymes, *AtHEMA2* and *AtFC1*, under stress conditions and their physiological functions in *Arabidopsis*. *Plant Physiol.* **144**, 1039–1051. (doi:10.1104/pp.107.100065)
- Scharfenberg M, Mittermayr L, Von Roepenack-Lahaye E, Schlicke H, Grimm B, Leister D, Kleine T. 2015 Functional characterization of the two ferrochelatases in *Arabidopsis thaliana*. *Plant Cell Environ.* **38**, 280–298. (doi:10.1111/pce.12248)
- Woodson JD, Joerns MS, Sinson AB, Gilkerson J, Salomé PA, Weigel D, Fitzpatrick JA, Chory J. 2015 Ubiquitin facilitates a quality-control pathway that removes damaged chloroplasts. *Science* **350**, 450–454. (doi:10.1126/science.aac7444)
- Espinás NA, Kobayashi K, Sato Y, Mochizuki N, Takahashi K, Tanaka R, Masuda T. 2016 Allocation of heme is differentially regulated by ferrochelatase isoforms in *Arabidopsis* cells. *Front. Plant Sci.* **7**, 1326. (doi:10.3389/fpls.2016.01326)
- Fan T, Roling L, Meiers A, Brings L, Ortega-Rodés P, Hedtke B, Grimm B. 2019 Complementation studies of the *Arabidopsis fc1* mutant substantiate essential functions of ferrochelatase 1 during embryogenesis and salt stress. *Plant Cell Environ.* **42**, 618–632. (doi:10.1111/pce.13448)
- Smith AG, Marsh O, Elder GH. 1993 Investigation of the subcellular location of the tetrapyrrole-biosynthesis enzyme coproporphyrinogen oxidase in higher plants. *Biochem. J.* **292**, 503–508. (doi:10.1042/bj2920503)
- Papenbrock J, Mishra S, Mock HP, Kruse E, Schmidt EK, Petersmann A, Braun HP, Grimm B. 2001 Impaired expression of the plastidic ferrochelatase by antisense RNA synthesis leads to a necrotic phenotype of transformed tobacco plants. *Plant J.* **28**, 41–50. (doi:10.1046/j.1365-313X.2001.01126)
- Cornah JE, Roper JM, Pal Singh D, Smith AG. 2002 Measurement of ferrochelatase activity using a novel assay suggests that plastids are the major site of haem biosynthesis in both photosynthetic and non-photosynthetic cells of pea (*Pisum sativum* L.). *Biochem. J.* **362**, 423–432. (doi:10.1042/bj3620423)
- Masuda T, Suzuki T, Shimada H, Ohta H, Takamiya K. 2003 Subcellular localization of two types of ferrochelatase in cucumber. *Planta* **217**, 602–609. (doi:10.1007/s00425-003-1019-2)
- Hey D, Ortega-Rodes P, Fan T, Schnurrer F, Brings L, Hedtke B, Grimm B. 2016 Transgenic tobacco lines expressing sense or antisense *FERROCHELATASE 1* RNA show modified ferrochelatase activity in roots and provide experimental evidence for dual localization of ferrochelatase 1. *Plant Cell Physiol.* **57**, 2576–2585. (doi:10.1093/pcp/pcw171)
- Chow KS, Singh DP, Roper JM, Smith AG. 1997 A single precursor protein for ferrochelatase-I from *Arabidopsis* is imported *in vitro* into both chloroplasts and mitochondria. *J. Biol. Chem.* **272**, 27 565–27 571. (doi:10.1074/jbc.272.44.27565)
- Suzuki T, Masuda T, Singh DP, Tan FC, Tsuchiya T, Shimada H, Ohta H, Smith AG, Takamiya K. 2002 Two types of ferrochelatase in photosynthetic and

- nonphotosynthetic tissues of cucumber: their difference in phylogeny, gene expression, and localization. *J. Biol. Chem.* **277**, 4731–4737. (doi:10.1074/jbc.M105613200)
37. Lister R, Chew O, Rudhe C, Lee MN, Whelan J. 2001 *Arabidopsis thaliana* ferrochelatase-I and -II are not imported into *Arabidopsis* mitochondria. *FEBS Lett.* **506**, 291–295. (doi:10.1016/S0014-5793(01)02925-8)
38. Leister D. 2005 Genomics-based dissection of the cross-talk of chloroplasts with the nucleus and mitochondria in *Arabidopsis*. *Gene* **354**, 110–116. (doi:10.1016/j.gene.2005.03.039)
39. Woodson JD, Chory J. 2008 Coordination of gene expression between organellar and nuclear genomes. *Nat. Rev. Genet.* **9**, 383–395. (doi:10.1038/nrg2348)
40. Pfanschmidt T. 2010 Plastidial retrograde signaling—a true ‘plastid factor’ or just metabolite signatures? *Trends Plant Sci.* **15**, 427–435. (doi:10.1016/j.tplants.2010.05.009)
41. Köhler RH, Cao J, Zipfel WR, Webb WW, Hanson MR. 1997 Exchange of protein molecules through connections between higher plant plastids. *Science* **276**, 2039–2042. (doi:10.1126/science.276.5321.2039)
42. Köhler RH, Zipfel WR, Webb WW, Hanson MR. 1997 The green fluorescent protein as a marker to visualize plant mitochondria *in vivo*. *Plant J.* **11**, 613–621. (doi:10.1046/j.1365-313X.1997.11030613.x)
43. Akashi K, Grandjean O, Small I. 1998 Potential dual targeting of an *Arabidopsis* archaeobacterial-like histidyl-tRNA synthetase to mitochondria and chloroplasts. *FEBS Lett.* **431**, 39–44. (doi:10.1016/S0014-5793(98)00717-0)
44. Emanuelsson O, Nielsen H, Brunak S, von Heijne G. 2000 Predicting subcellular localization of proteins based on their N-terminal amino acid sequence. *J. Mol. Biol.* **300**, 1005–1016. (doi:10.1016/j.cell.2008.06.016)
45. Nielsen H, Engelbrecht J, Brunak S, von Heijne G. 1997 Identification of prokaryotic and eukaryotic signal peptides and prediction of their cleavage sites. *Protein Eng.* **10**, 1–6. (doi:10.1093/protein/10.1.1)
46. Cerutti H, Osman M, Grandoni P, Jagendorf AT. 1992 A homolog of *Escherichia coli* RecA protein in plastids of higher plants. *Proc. Natl Acad. Sci. USA* **89**, 8068–8072. (doi:10.1073/pnas.89.17.8068)
47. Maarse AC, Van Loon AP, Riezman H, Gregor I, Schatz G, Grivell LA. 1984 Subunit IV of yeast cytochrome c oxidase: cloning and nucleotide sequencing of the gene and partial amino acid sequencing of the mature protein. *EMBO J.* **3**, 2831–2837. (doi:10.1002/j.1460-2075.1984.tb02216)
48. Nakagawa T *et al.* 2007 Improved gateway binary vectors: high-performance vectors for creation of fusion constructs in transgenic analysis of plants. *Biosci. Biotech. Biochem.* **71**, 2095–2100. (doi:10.1271/bbb.70216)
49. Clough SJ, Bent AF. 1998 Floral dip: a simplified method for *Agrobacterium*-mediated transformation of *Arabidopsis thaliana*. *Plant J.* **16**, 735–743. (doi:10.1046/j.1365-313x.1998.00343)
50. Harrison SJ, Mott EK, Parsley K, Aspinnall S, Gray JC, Cottage A. 2006 A rapid and robust method of identifying transformed *Arabidopsis thaliana* seedlings following floral dip transformation. *Plant Methods* **2**, 19. (doi:10.1186/1746-4811-2-19)
51. Page MT, McCormac AC, Smith AG, Terry MJ. 2017 Singlet oxygen initiates a plastid signal controlling photosynthetic gene expression. *New Phytol.* **213**, 1168–1180. (doi:10.1111/nph.14223)
52. Bustin SA *et al.* 2009 The MIQE guidelines: minimum information for publication of quantitative real-time PCR experiments. *Clin. Chem.* **55**, 611–622. (doi:10.1373/clinchem.2008.112797)
53. Lichtenthaler HK, Buschmann C. 2001 Chlorophylls and carotenoids: measurement and characterization by UV-VIS spectroscopy. *Curr. Protoc. Food Anal. Chem.* **1**, F4.3.1–F4.3.8. (doi:10.1002/0471142913.faf0403s01)
54. Terry MJ, Kacprzak SM. 2019 A simple method for quantification of protochlorophyllide in etiolated *Arabidopsis* seedlings. In *Phytochromes: methods and protocols, methods in molecular biology*, vol. 2026. (ed. A Hiltbrunner), pp. 169–177. New York, NY: Springer Nature. (doi:10.1007/978-1-4939-9612-4_14)
55. Armbruster U *et al.* 2009 Chloroplast proteins without cleavable transit peptides: rare exceptions or a major constituent of the chloroplast proteome? *Mol. Plant* **2**, 1325–1335. (doi:10.1093/mp/ssp082)
56. Bölter B, Nada A, Fulgosi H, Söll J. 2006 A chloroplastic inner envelope membrane protease is essential for plant development. *FEBS Lett.* **580**, 789–794. (doi:10.1016/j.febslet.2005.12.098)
57. Elortza F, Mohammed S, Bunkenborg J, Foster LJ, Nühse TS, Brodbeck U, Peck SC, Jensen ON. 2006 Modification-specific proteomics of plasma membrane proteins: identification and characterization of glycosylphosphatidylinositol-anchored proteins released upon phospholipase D treatment. *J. Prot. Res.* **5**, 935–943. (doi:10.1021/pr050419u)
58. Aryal N, Lu C. 2018 A phospholipase C-like protein from *Ricinus communis* increases hydroxy fatty acids accumulation in transgenic seeds of *Camelina sativa*. *Front. Plant Sci.* **9**, 1576. (doi:10.3389/fpls.2018.01576)
59. Itoh RD, Yamasaki H, Septiana A, Yoshida S, Fujiwara MT. 2010 Chemical induction of rapid and reversible plastid filamentation in *Arabidopsis thaliana* roots. *Physiol. Plant.* **139**, 144–158. (doi:10.1111/j.1399-3054.2010.01352)
60. McCormac AC, Terry MJ. 2004 The nuclear genes *Lhcb* and *HEMA1* are differentially sensitive to plastid signals and suggest distinct roles for the GUN1 and GUN5 plastid-signalling pathways during de-etiolation. *Plant J.* **40**, 672–685. (doi:10.1111/j.1365-313X.2004.02243.x)
61. Terry MJ, Kendrick RE. 1999 Feedback inhibition of chlorophyll synthesis in the phytochrome chromophore-deficient *aurea* and *yellow-green-2* mutants of tomato. *Plant Physiol.* **119**, 143–152. (doi:10.1104/pp.119.1.143)
62. Terry MJ, Ryberg M, Raitt CE, Page AM. 2001 Altered etioplast development in phytochrome chromophore-deficient mutants. *Planta* **214**, 314–325. (doi:10.1007/s004250100624)
63. Goslings D, Meskauskiene R, Kim C, Lee KP, Nater M, Apel K. 2004 Concurrent interactions of heme and FLU with glu tRNA reductase (HEMA1), the target of metabolic feedback inhibition of tetrapyrrole biosynthesis, in dark- and light-grown *Arabidopsis* plants. *Plant J.* **40**, 957–967. (doi:10.1111/j.1365-313X.2004.02262.x)
64. Richter AS, Banse C, Grimm B. 2019 The GluTR-binding protein is the heme-binding factor for feedback control of glutamyl-tRNA reductase. *eLife* **8**, e46300. (doi:10.7554/eLife.46300)
65. Terry MJ, Bampton J. 2019 The role of tetrapyrroles in chloroplast-to-nucleus retrograde signalling. *Adv. Bot. Res.* **91**, 225–246. (doi:10.1016/bs.abr.2019.05.002)
66. Larkin RM. 2016 Tetrapyrrole signaling in plants. *Front. Plant Sci.* **7**, 1586. (doi:10.3389/fpls.2016.01586)
67. Tadini L *et al.* 2016 GUN1 controls accumulation of the plastid ribosomal protein S1 at the protein level and interacts with proteins involved in plastid protein homeostasis. *Plant Physiol.* **170**, 1817–1830. (doi:10.1104/pp.15.02033)
68. Llamas E, Pulido P, Rodriguez-Concepcion M. 2017 Interference with plastome gene expression and Clp protease activity in *Arabidopsis* triggers a chloroplast unfolded protein response to restore protein homeostasis. *PLoS Genet.* **13**, e1007022. (doi:10.1371/journal.pgen.1007022)
69. Marino G, Naranjo B, Wang J, Penzler J-F, Kleine T, Leister D. 2019 Relationship of GUN1 to FUG1 in chloroplast protein homeostasis. *Plant J.* **99**, 521–535. (doi:10.1111/tpj.14342)
70. Zhao X, Huang J, Chory J. 2019 GUN1 interacts with MORF2 to regulate plastid RNA editing during retrograde signalling. *Proc. Natl Acad. Sci. USA* **116**, 10 162–10 167. (doi:10.1073/pnas.1820426116)
71. Wu GZ *et al.* 2019 Control of retrograde signalling by protein import and cytosolic folding stress. *Nat. Plants* **5**, 525–538. (doi:10.1038/s41477-019-0415)
72. Shimizu T *et al.* 2019 The retrograde signalling protein GUN1 regulates tetrapyrrole biosynthesis. *Proc. Natl Acad. Sci. USA* **116**, 24 900–24 906. (doi:10.1073/pnas.1911251116)